Experimental Thermal and Fluid Science 63 (2015) 106–114

Contents lists available at ScienceDirect

Experimental Thermal and Fluid Science

journal homepage: www.elsevier.com/locate/etfs

Critical heat flux of cyclohexane in uniformly heated minichannels with high inlet subcooling

Zhaohui Liu, Qincheng Bi *, Zhuqiang Yang, Yong Guo, Jianguo Yan

State Key Laboratory of Multiphase Flow in Power Engineering, Xi'an Jiaotong University, Xi'an 710049, PR China

ARTICLE INFO

Article history:
Received 20 October 2014
Received in revised form 22 January 2015
Accepted 22 January 2015
Available online 30 January 2015

Keywords:
CHF
Inlet subcooling
Hydrocarbons
Cyclohexane
Minichannel

ABSTRACT

The critical heat flux (CHF) for flow boiling of cyclohexane was experimentally investigated in electrically heated minichannels with inside diameters of (1 and 2) mm, and heated lengths of (360 and 710) mm at mass velocities ranging from (318 to 1274) kg/m^2 s, heat fluxes from (50 to 1000) kW/m^2, and pressures of (1.0, 2.0, 3.0) MPa. Cyclohexane entered the test channel at ambient temperature of about 20 °C, equivalent to high subcooling of (162.1, 206.4 and 236.3) °C at (1.0, 2.0 and 3.0) MPa respectively. The critical vapor qualities ranged from −1.35 to 0.83. Results indicated that CHF of cyclohexane increased with increasing mass velocity and decreasing heated length. Reducing channel diameter at the same length-to-diameter ratio was proved to have no effects on CHF values of cyclohexane at the evaluated conditions. CHF mildly increased with an increase in pressure at higher mass velocities, but critical vapor quality always decreased with the increasing pressure. Experimental CHF data were compared with the Katto–Ohno (1984) correlation and Shah (1987) correlation. Good agreements were achieved between the experimental data and those predicted with most deviations not exceeding 30%. A corrected Katto–Ohno CHF correlation is developed to fit the current experimental data. Excellent agreement was obtained with all the deviations (whatever of saturation CHF or subcooled CHF) in the range of ±10% with RMS error of 5.35%.

1. Introduction

The mini/micro channels are becoming widely used as heat sinks in thermal management system [1] such as aerospace flight [2], electrical cooling devices [3,4], and refrigeration systems [5,6] in the recent decades. The space and/or weight constraints in the small scale devices make the cooling channel much tinier, and also the small passages may provide a high performance. The flow boiling heat transfer processes are usually used in the high heat flux removal applications. Therefore the CHF prediction is of vital importance for the safe operation of heat dissipation applications.

CHF has been widely researched since the period of 1940 [7]. But there is considerable confusion about its trigger mechanism, experimental detection and prediction. Though a vast number of CHF data and empirical correlations are available in literatures, two phase designers are often confronted with great difficulty predicting CHF with acceptable accuracy. The primary reason [7] is the special case of flow boiling in tubes, including special fluids, flow geometries and operating conditions.

Flow boiling heat transfer deterioration at CHF condition always appears as a sudden increase of the surface temperature and appreciable reduction in local heat transfer coefficient resulting from inadequate liquid access to the wall, which may bring a severe danger or even destroy the cooled devices. CHF always occurs at channel outlet. As heat flux continues to increase after the occurrence of CHF, the heat transfer deterioration shifts forward to the front of the channel. According to the different channel heated lengths, channel diameters, inlet subcoolings, mass velocities and pressures, CHF can occur at different vapor qualities. Depending on the quality greater than zero or not, CHF can be classified as saturated CHF or subcooled CHF.

The typical dryout type CHF was seen in the high-quality saturated region when the two-phase flow pattern is completely annular. The annular flow patterns in the visualization study of Kosar and Peles [4] and Kosar et al. [8] indicated that dryout is the saturated CHF mechanism in micro/mini-channels. It is important to accurately predict CHF in saturated conditions in small diameter channels. Katto [9] developed a generalized dimensionless correlation of saturated CHF for any arbitrary fluid, mass velocity, tube diameter and length, and the inlet subcooling. An improved version of the correlation by Katto and Ohno [5] was published and based on the division of CHF regime by

* Corresponding author. Tel./fax: +86 (0)29 82665287.
E-mail address: qcbi@mail.xjtu.edu.cn (Q. Bi).

http://dx.doi.org/10.1016/j.expthermflusci.2015.01.012
0894-1777/

Nomenclature

Bl	boiling number, $q/(Gh_{lv})$ (−)
D	inside channel diameter (m)
G	mass velocity of liquid plus vapor (kg/m^2 s)
h	enthalpy (J/kg)
I	electricity current (A)
L	heated length (m)
M	mass flow rate (g/s)
P	pressure (MPa)
q	local heat flux (W/m^2)
Q	total power applied to the test section (W)
T	temperature (°C)
U	voltage (V)
x	vapor quality (−)

Greek symbols

ρ	density (kg/m^3)
σ	surface tension (N/m)

Subscripts

c	critical
exp	experimental
l	liquid
lv	liquid–vapor
pre	predicted
s	saturation
v	vapor
w	wall

$\rho_V/\rho_L = 0.15$ in order to discriminate the high pressure regime from others. Qu and Mudawar [3] found that this correlation is fairly accurate at predicting saturated CHF in single circular minichannels. Shah [10] proposed a new version of his previous correlation to predict CHF during upflow in uniformly heated vertical tubes under saturated and subcooled conditions. Even more accuracy was found of this method by shah when comparing with Katto and Ohno correlation. There are also some other famous correlations reported by Qu and Mudawar [3], Wojtan [11], and Zhang [12].

Parametric effects on CHF in mini/micro channel were studied in many experiments in the past decade. CHF will be mainly influenced by mass velocity, heated length, saturation temperature, channel diameter, inlet liquid subcooling and fluid thermal properties. It was generally found that CHF decreased with an increase in heated length in the microchannel [11,13,14], and the length-to-diameter ratio was always involved in the CHF predicted correlations. Bigger CHF always was found at higher mass velocity [3,4,13]. To our knowledge, no literatures reported opposite effects of mass velocity on CHF.

The diameter and pressure effects on CHF are much more complex. Tanase and Groeneveld [15] proposed a diameter correction correlation to equivalently derive CHF in different diameter channels from a given CHF value in a certain diameter channel, which was widely used to establish a CHF lookup table [16]. But the constant term in the diameter correction correlation was reported different in literatures [15]. Some recent literatures of Thome [6,17] reported that the diameter had no significant effects on CHF of R134a and R236fa until the mass velocity went up to 500 kg/m^{2}s.

It seems that pressure effect on CHF in mini/microchannel is in some degree dependent on the working fluid. For water, Roday and Jensen [13] reported that CHF increases with an increase in pressure for a constant inlet subcooling. Wojtan [11] reported no significant differences in CHF for both saturation temperature of 30 °C and 35 °C of R134a at mass velocity lower than 1000 kg/m^2 s, but for higher mass velocity CHF increased with saturation temperature (increase in pressure). Thome [6,17] reported different results that CHF of R134a, R236fa and R245fa decreased with increasing saturation temperature at higher mass velocities. Kosar [4] reported that increasing pressure leaded to an increase in CHF values of R123 up to a certain pressure, beyond which CHF declined.

Effect of inlet subcooling was investigated. In terms of refrigerates many literatures concentrated on, wide range of liquid inlet subcooling are often not investigated because large subcoolings are usually not easy to acquire while saturation temperature is only tens centigrade above ambient temperature. These limited experimental data showed that CHF did not change significantly for the limited subcoolings. Wojtan et al. [11] shows no significant influences of inlet subcooling ranging from 4.5 to 12 °C on CHF for R134a while T_{sat} = 35 °C. Qu and Mudawar [3] investigated CHF of a water-cooled microchannel heat sinks at inlet temperature of 30 °C and 60 °C at an outlet pressure of 1.13 bar. As CHF was approached, flow instabilities induced vapor backflow which significantly altered the coolant temperature at the channel inlets, resulting in a CHF virtually independent of inlet temperature.

Before the use of minichannels under flow boiling condition, it is essential to understand the CHF mechanism and predict CHF accurately. In this study a series of experimental CHF tests for single, uniformly heated minichannels with (1 and 2) mm ID have been undertaken using cyclohexane as working fluid. The main objectives of this work are (a) to determine the influence of mass velocity, heated length, channel diameter, pressure, and inlet subcooling on CHF of cyclohexane in single minichannels; (b) to develop suitable CHF correlation for cyclohexane. The results of this paper will offer valuable information for the thermal design of cooling structures which refers to the CHF of hydrocarbons in minichannels.

2. Experiments

2.1. Experimental setup

The flow boiling CHF of cyclohexane was experimentally investigated in nickel alloy GH3128 [18] (Chinese standard) electrically heated horizontal minichannels (heated length L_h: 360 mm, 710 mm; inside diameter D: 1.0 mm, 2.0 mm; wall thickness: 0.5 mm) which can work well at temperature up to 1000 °C. Therefore the test channel would not be damaged by CHF, which provided the possibility to investigate CHF behavior by continuing to increase heat flux after the occurrence of CHF. The average roughness (Ra) of the test channel inner surface was measured as 0.8 μm by 3D measuring Laser Microscope Olympus LEXT OLS4000. The purity of cyclohexane used is larger than 99.5% in mass fraction. The schematic diagram of the experimental apparatus is shown in Fig. 1. The experimental facilities and the test section were described in detail by our previous reports [19–21].

The fluid inlet and outlet temperature of the test channel were measured by type K sheathed thermocouples with outside diameter of 1.0 mm, which were immerged into the flow passage. Some 15 thermocouples (TC) of type K with outside diameter of 0.2 mm were spot-welded on bottom surface of the channel with intervals of 25 mm to measure the outside wall temperature, from which

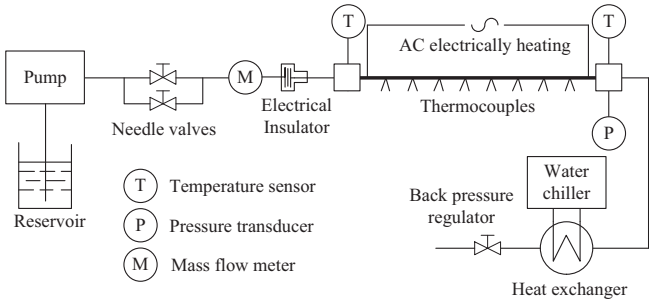

Fig. 1. Schematic diagram of experimental apparatus.

the inside wall temperatures were derived. The test channels were wrapped by thermal insulation cotton to reduce heat losses.

The cyclohexane flow was provided precisely by a constant volume pump (Elite P500 from China) with flow stability of ±0.5%. A Coriolis mass flow meter before the test channel was used to measure the real time mass flow rate. The outlet pressure and pressure drop across the test section were measured by Rosemont 3051 transducers. All measured data were collected by Isolated Measurement Pods 3595 (IMP3595) data acquisition system.

2.2. Data reduction and experimental validation

All the heat flux referred in this paper is local heat flux obtained by the Eq. (1), in which the heat efficiency η as a function of the channel outside wall temperature was measured by the heat balance method. The Joule heat generated in the channel was balanced with the heat loss to the ambience while no working fluid was employed.

$$q = UI\eta/\pi DL \tag{1}$$

The nearly uniform heat fluxes along the test channel would be a little different, because that the heat losses differed at different wall temperatures. But the discrepancy was less than 5.0% at a wide range of temperatures from ambient to 800 °C.

The local fluid enthalpy at the ith TC points h_i was obtained by the Eq. (2), where h_{inlet} denotes the enthalpy of the inlet liquid cyclohexane, and L_i denotes the distance of the ith TC away from the entrance of the test channel. The local vapor quality was calculated from the local fluid enthalpy. All the thermal properties of cyclohexane are referred from the NIST REFPROP program.

$$h_i = 1000\frac{UI\eta}{M}\frac{L_i}{L} + h_{\text{inlet}} \tag{2}$$

The inside wall temperature at each TC point was determined by deducting the calculated temperature drop through the wall, the equation of which was referred from [22].

In this paper, at each operation condition of a given mass flow rate, pressure, channel length and diameter, the heating power was controlled to increase step by step from $q = 0$ until the working fluid were completely vaporized (vapor quality larger than 1). The channel outlet fluid was controlled to increase from ambient temperature to superheating. During this process, the experiments achieved steady states at all steps amongst which there was one step the CHF occurred. The experimental data were collected at every plateau while the outlet fluid experienced single phase liquid flow, liquid–vapor two phase flow and single phase vapor flow. The accuracy of the estimated vapor quality was assured by both the single phase liquid and single phase vapor flow experiments. A new test channel was used for each operation condition. Repeated experiments were conducted at each operation condition by changing the test channel. Good repeatability was confirmed that all the repeated experiment results fell in the range of the standard uncertainties.

Table 1
Uncertainties of the main parameters.

Parameters	Uncertainties (%)
Heat flux q	±2.2
Mass velocity G	±3.0
Fluid enthalpy h	±1.3
Vapor quality x	±4.0
Critical heat flux q_c	±7.2
Critical vapor quality x_c	±9.2

The expanded standard uncertainties of the measured and derived data were listed in Table 1. All the uncertainties were estimated in 95% confidence level by using a coverage factor of 2. The standard uncertainties of the thermocouples are ±0.2 °C at temperature $T < 200$ °C, ±0.5 °C at $200\ °C \leqslant T < 500$ °C, and ±1.0 °Cat $500\ °C \leqslant T < 800$ °C. The discontinuous heat flux increase during the experiment introduced additional uncertainties of ±5.0% for the critical heat flux and critical vapor quality, which have been considered in the Table 1.

3. Results and discussions

In this paper CHF of cyclohexane was investigated in the uniformly heated minichannel at mass velocity ranging from (318 to 2547) kg/m^2 s, heat flux from (50 to 1000) kW/m^2, reduced pressure of approximately (0.25, 0.5 and 0.75). The highly subcooled cyclohexane entered the test channel at ambient temperature of about 20 °C, equivalent to high subcooling of (162.1, 206.4 and 236.3) °C at (1.0, 2.0 and 3.0) MPa respectively.

3.1. Flow boiling heat transfer deterioration and CHF of cyclohexane

Fig. 2 shows the wall temperature profiles along the heated channel at different heat fluxes. Heat transfer deterioration (HTD[1]) was clearly indicated as the appreciated temperature rise (ATR[2]) along the channel in Fig. 2(a) or with the increasing heat flux in Fig. 2(b). Before ATR the wall temperature slightly above the fluid saturation temperature kept nearly constant along the test channel and hardly increased with the increasing heat flux, which are the characteristics of nucleate boiling. The convective heat transfer enhanced by flow boiling appears in such a way that the temperatures at the tube interior surface remain approximately constant up to the boiling crisis. And as long as the heating surface is wetted, the wall temperatures are only insignificantly higher than the fluid saturation temperature T_s=182.07 °C at P = 1 MPa.

The onset of CHF is characterized by a drastic increase in wall temperature, and the convective flow deviated from nucleation boiling to dryout in the saturation boiling or burnout in the subcooled boiling. Dryout is indicated as the saturated CHF mechanism [4], and burnout (or film boiling, DNB) is the mechanism of subcooled CHF. CHF always occurs at channel outlet. As shown in Fig. 2, wall temperature TC15 at the channel outlet started deviating the boiling region and increased appreciably at heat flux q = 429 kW/m^2, where the maximum heat flux to maintain the wall temperature at nucleation boiling condition is marked as CHF.

Dedicated to the high temperature performance of GH3128 minichannel used, the test channels were not destroyed by CHF in all the operations. By continuing to increase the heat flux after the occurrence of CHF, the behaviors of HTD initiated from CHF were reported. At post-CHF regime [23] the heating surface is

[1] HTD: Heat transfer deterioration.
[2] ATR: appreciated temperature rise.

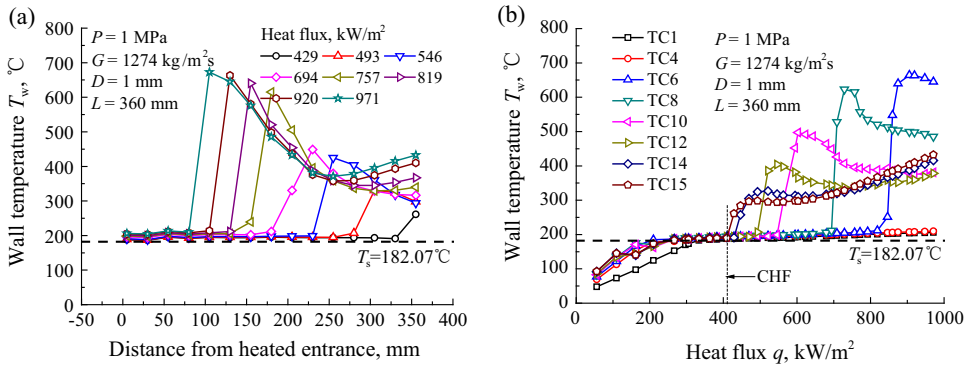

Fig. 2. Profiles of wall temperature (a) along the heated channel at different heat fluxes and (b) with heat flux for different TC points.

not wetted, and the heat from the channel wall is transferred directly to the gas phase. Due to the lower heat transfer coefficient of gas phase, heat transfer in this regime is considerably reduced. Therefore significantly higher wall temperatures are expected than with a wetted channel wall.

As heat flux continued to increase, ATR (onset of heat transfer deterioration) shifted toward the front TC points on the channel. Meanwhile, higher wall temperatures are shown in the front of the channel after the onset of CHF. The temperature rise is less than 100 °C at $q = 429\ kW/m^2$, but increases to over 450 °C at $q = 971\ kW/m^2$. Heat transfer deterioration along the channel is as a result of the unwetted channel wall, which is called post-Dryout regime. The quality at the dryout location profoundly affects the level of post-Dryout wall temperatures. If the dryout occurs at low qualities, higher wall temperatures must be expected than if the channel dries out at high qualities. One reason for this is that the average flow velocity rises with increasing quality, thus enhancing the cooling performance at the channel interior surface. And another reason here is the higher heat flux imposed while dryout occurs at lower quality or lower bulk fluid temperature region.

3.2. Method of detecting dryout condition along the heated channel

As heat flux continued to increase after the occurrence of CHF (the first case of dryout), dryout shifted toward the front TC points on the channel. Dryout conditions along the heated channel are investigated to aid CHF research. There are different methods for CHF detection and measurement. Following are the popular methods [7]: (a) first measureable degradation in flow boiling heat transfer, indicated by a slope change of the upper portion of the nucleate boiling curve; (b) rise in heated wall temperature above a fixed level indicated by the experimenter; (c) appreciable temperature rise of any portion of the heated wall; (d) increasing heat flux until the wall temperature escalates uncontrollably.

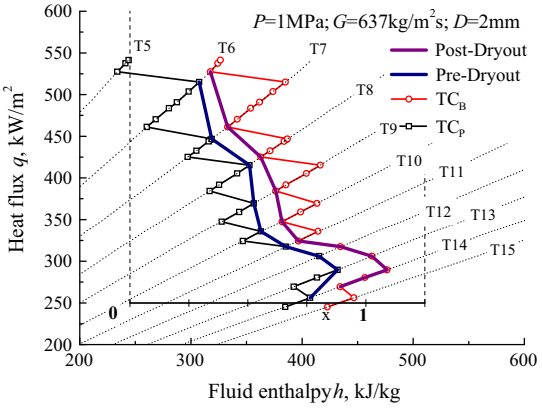

Fig. 3. Detection of local dryout condition in the map of fluid states presented by heat flux vs. enthalpy.

In this study there are always 15 thermocouples distributed along the test channel. ATR at each TC was recognized as the characteristic of dryout at the location. Fig. 3 shows the detection of dryout condition, in which the corresponding heat flux and fluid enthalpy are indicated for each dryout location along the test channel. That the fluid enthalpy increased with increasing heat flux is showed as dash line from TC5 to TC15. The TC points with ATR along the channel (at the same heat flux) are marked as red color point and the one before is marked as black point. At low heat flux region ATR first appeared at TC15, which is recognized as CHF. As heat flux continued to increase after the occurrence of CHF, ATR could shift forward to the front TC along the channel. However, sometimes it would not shift to the front TC point until considerable heat flux increment was imposed. An exemplification is the HTD between T6 and T7 at heat flux from (460 to 515) kW/m^2. Obviously in the area between the red curve (TC_B) and the black curve (TC_p) the dryout took place.

However, as heat flux increased there was only one onset condition of dryout with ATR for each thermocouple, which makes up the post-Dryout curve (the purple curve in Fig. 3) for the whole test channel. And the black points just before the red one (on the purple curve) for all the TC points made up the pre-Dryout curve (the blue curve in Fig. 3). Obviously at heat flux larger than CHF, the dryout conditions along the test channel were contracted to the region between the post-Dryout curve and pre-Dryout curve. And we assume that the pre-Dryout curve is the dryout condition curve which will be used in the following parts of the paper.

It can be clearly seen that the vapor quality of the flow at the dryout condition reduced with increasing heat flux, and higher wall temperatures should be expected than if the channel dries out at high qualities. That is why the temperature rise rate for DNB at low quality or subcooled liquid is bigger than the dryout at high quality condition. And that makes the DNB more dangerous than dryout type CHF.

3.3. Effect of mass velocity on CHF

Fig. 4 shows the CHF and dryout profiles at different mass velocities for different pressures and channel diameters. The dryout vapor qualities detected by the approach described in Section 3.2 are shown to linearly reduce with increasing heat flux in all the figures. As well as in Fig. 4(a), CHF points shown in all the figures are the left-most point of every line fitted, for CHF occurring as the initial dryout in the test channel. There exists a trend in nearly all the dryout fitting lines that dryout vapor quality reduced with the

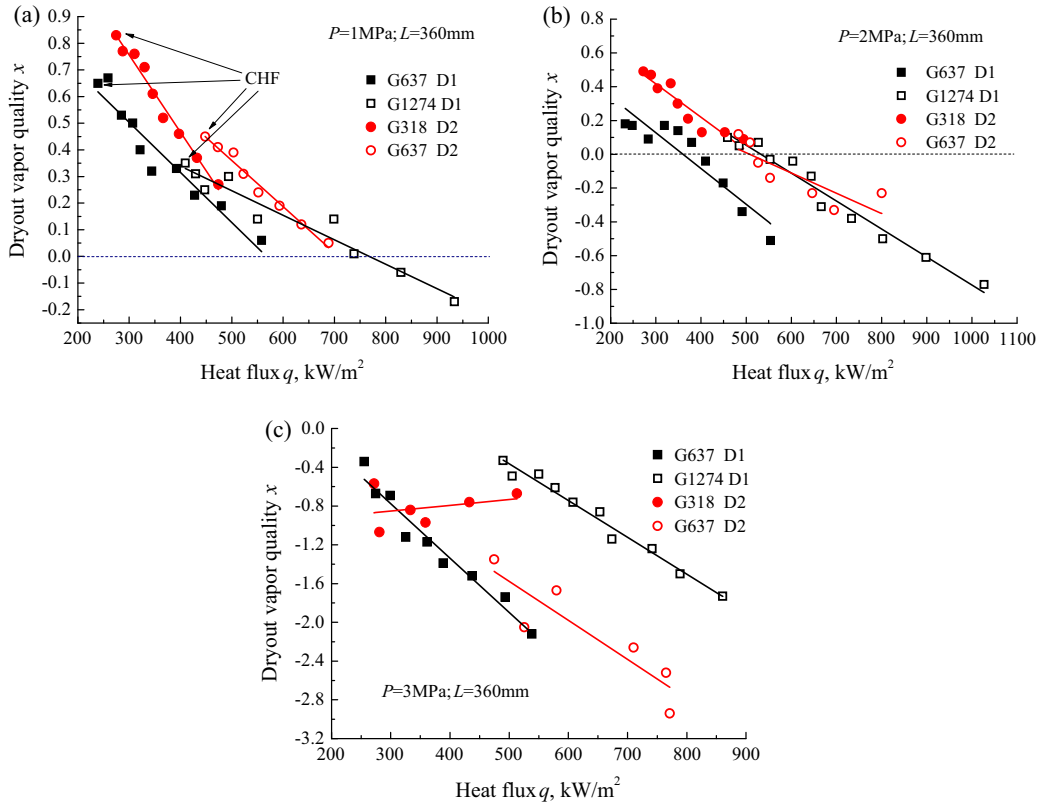

Fig. 4. Variation of dryout vapor quality with heat flux for different channels and mass fluxes. G is mass velocity, and D is channel inside diameter.

Table 2
CHF values at different mass velocities (L = 360 mm).

D (mm)	1			2		
P (MPa)	1	2	3	1	2	3
G = 318 kg/m^2 s	–	–	–	274.8	272.5	271.9
G = 637 kg/m^2 s	239.1	232.4	255.0	448.2	483.1	474.6
G = 1274 kg/m^2 s	409.3	458.8	489.8	–	–	–

increasing heat flux. Moreover all the lines move to the low quality region or even subcooled region at higher pressures, which indicated that dryout vapor quality reduced with an increase in pressure.

All the CHF values in Fig. 4 are summarized in Table 2. It indicates that CHF of cyclohexane increased with an increase in mass velocity at all the operation conditions. For the 2 mm ID channel, the CHF values at G = 637 kg/m^2 s are nearly twice bigger than that at G = 318 kg/m^2 s at all the pressures of (1, 2 and 3) MPa. And it is the same case for 1 mm ID channel between G = 1274 and G = 637 kg/m^2 s. Previous investigations [3,13] reported the CHF dependence on mass velocity for different working fluids.

If CHF values were doubled while the mass velocity doubled, the critical vapor quality should be constant. But it is noticed in Table 2 that all the CHF values at bigger G were nearly but less than twice of those at smaller G. It indicates that CHF shifted to lower vapor quality condition at bigger mass velocity, which was validated in Table 3.

Table 3
Critical vapor qualities at different mass velocities (L = 360 mm).

D (mm)	1			2		
P (MPa)	1	2	3	1	2	3
G = 318 kg/m^2 s	–	–	–	0.83	0.49	−0.57
G = 637 kg/m^2 s	0.65	0.18	−0.34	0.45	0.12	−1.35
G = 1274 kg/m^2 s	0.35	0.1	−0.49	–	–	–

3.4. Effect of Length-to-diameter ratio on CHF

Length-to-diameter ratio L/D is generally introduced in the CHF correlations [3,5], in which constant coefficient is always different for different L/D regions. Boiling number at CHF Bl_c as a function of L/D was described [14] basing on CHF data collected from literatures. Bl_c decreases greatly with a small increase in length-to-diameter ratio L/D when $L/D \leqslant 50$. A relatively smooth trend occurs when $L/D > 150$. A transition appears in the region $50 < L/D \leqslant 150$.

In this study length-to-diameter ratio L/D ranges of 180–360. Comparison of CHF and dryout data was shown in Fig. 5 for 2 mm ID channel with different heated length of (360 and 710) mm at pressures of (1, 2 and 3) MPa. Results well agreed with the literatures. CHF (left-most point) at the same mass velocity decreased with an increase in heated length from (360 to 710) mm at all the pressures. The dryout condition lines also support the same trend of CHF. Comparison of CHF at different length-to-diameter ratios are given in Table 4. As heated length doubled, CHF nearly half reduced.

3.5. Effects of diameter and pressure on CHF

The CHF and dryout data at different channel diameters are shown in Fig. 6 at G = 637 kg/m^2 s, and $L/D \approx 360$. The CHF and critical vapor quality values are listed in Table 5. The CHF values had no significant increases with a reduction in channel diameter to 1 mm from 2 mm at all tested pressures, which is different with previous literatures [15] which concluded that CHF generally decreases with increasing channel diameter at the same local

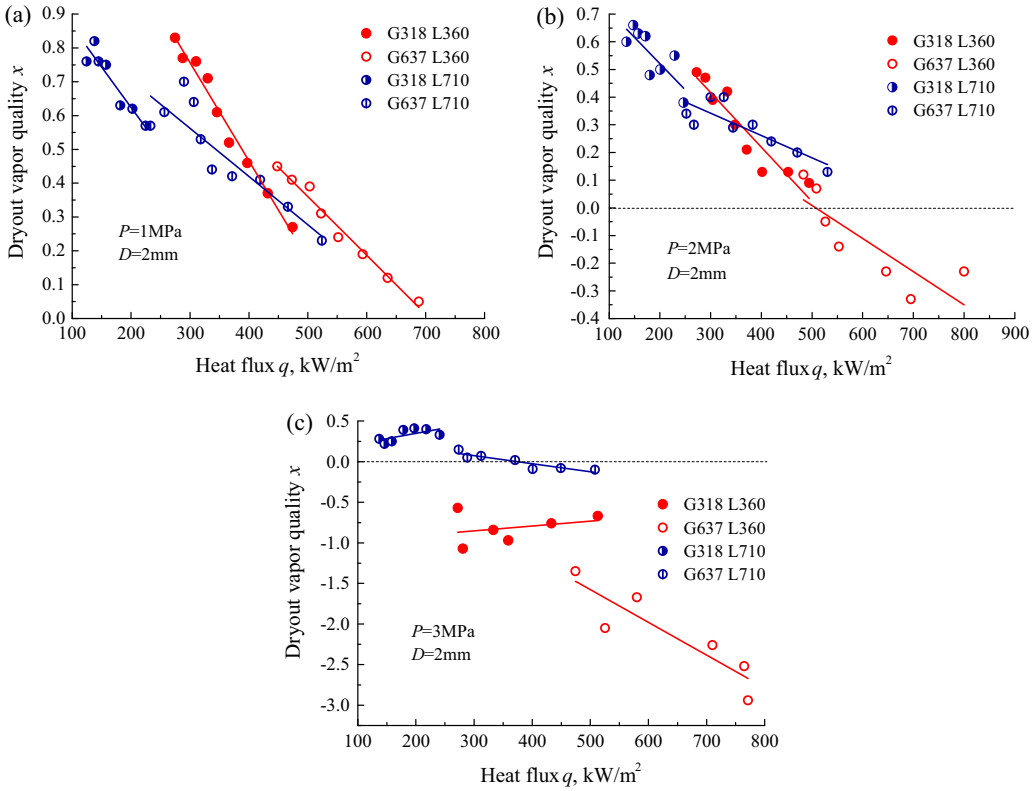

Fig. 5. Comparison of CHF and dryout data in 2 mm ID channel with different heated lengths of 360 mm and 710 mm.

Table 4
Variation of CHF values in channel with 2 mm ID and different heated lengths.

L_h (mm)	360			710		
P (MPa)	1	2	3	1	2	3
G = 318 kg/m^2 s	274.8	272.5	271.9	124.4	134.3	136.8
G = 637 kg/m^2 s	448.2	483.1	474.6	233	252.2	273.6

Table 5
Effect of diameter and pressure on CHF (L/D≈360, G = 637 kg/m^2 s).

D (mm)	1			2		
P (MPa)	1	2	3	1	2	3
q_c (kW/m^2)	239.1	232.4	255.0	233	252.2	273.6
x_c	0.65	0.18	−0.34	0.57	0.34	0.15

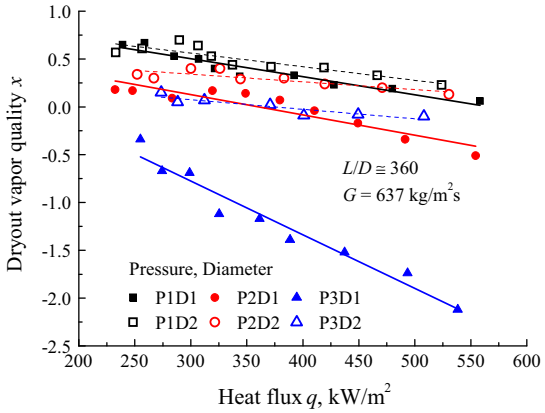

Fig. 6. Effect of diameter and pressure on CHF and dryout condition. P is pressure and D is channel inside diameter.

conditions. CHF was reported and evaluated by numerous previous literatures about CHF correlations [1,3,5] and CHF lookup table [16]. Different authors [15] have proposed several types of correlations or factors to describe the diameter effect on CHF. And for $3 < D < 25$ mm, P = 100–20,000 kPa, G = 0–8000 kg/m^2 s and $x_c = -0.5$ to 1, the CHF can be predicated by Eq. (3). It can be derived that CHF at 1 mm channel will be 1.44 times bigger than that at 2 mm channel according to the equation. Results indicate that the equation is not appropriate for CHF of cyclohexane in 1 mm and 2 mm channels.

$$\frac{(q_c)_D}{(q_c)_{D=8\text{ mm}}} = \left(\frac{8}{D}\right)^{1/2} \tag{3}$$

But in the recent literature of Ong and Thome [17] it reported a similar result that there is no channel size effects on the CHF of R134a and R236fa for the mass velocity range of up to G = 500 kg/m^2 s. Above G = 500 kg/m^2 s, the CHF values diverge and increase with an decrease in diameter from 3.04 mm to 1.03 mm.

Pressure had complex effects on the CHF. Experimental results in Table 5 showed that CHF mildly increased and the critical vapor quality decreased with an increase in pressure. Moreover, at higher mass velocities (showed in Table 2) the CHF increase became more obvious. Fig. 7 summarized and separated the dryout points including CHF at different pressures for all the operation conditions. It indicated that increasing pressure leaded to lower dryout vapor quality. Though higher saturation temperature occurred at higher pressure, the HTD can happen at lower fluid temperature, seen in Fig. 7(b). No instabilities resulting from pressure fluctuation were observed. And most deviations of pressure values from the mean were in the range of ±0.01 MPa. Therefore all the CHF data were collected at steady states without instability.

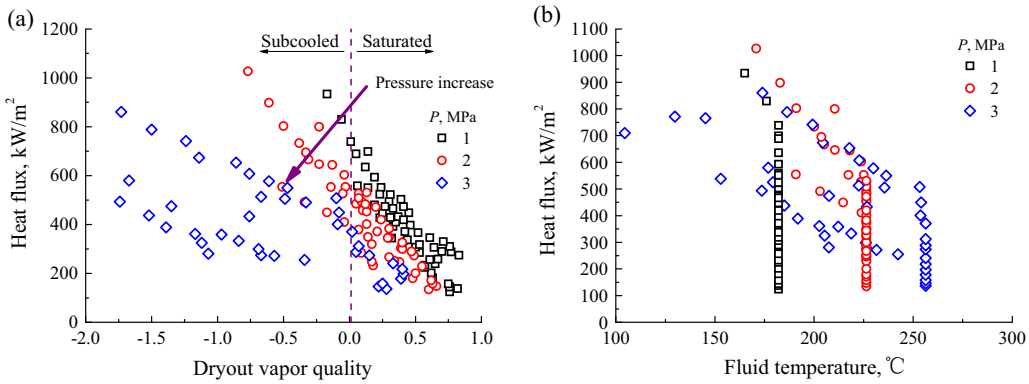

Fig. 7. Pressure effect on dryout vapor quality and dryout temperature. All the data points for different heated lengths, channel diameters, mass velocities in Figs. 4 and 5 are included.

Similar trend was found by Roday and Jensen [13] that CHF of water was nearly doubled while the absolute pressure increased from 25.3 kPa to 179 kPa in a microchannel with diameter of 0.427 mm. But the recent literature of Tibirica and Thome [6] found a completely opposite effect of pressure on CHF of R134a. They concluded that the CHF decreased with increasing saturation temperature and explained that this fact can be associated mainly with the decrease in the latent heat of vaporization with the increasing saturation temperature. However, there existed a common result that the CHF difference (whatever increase in this paper or decrease in Tibirica and Thome's report [6]) enlarged at higher mass velocities. It is clear that the explanation by latent heat of vaporization is not applicable for CHF of cyclohexane here. Even though less latent heat of vaporization is needed at higher pressure in fact and the critical vapor quality is also less (shown in Table 5), the CHF still in some degree increased with an increase in pressure at higher mass velocities.

3.6. A simply fitted qualitative CHF correlation

It was noticed that CHF was nearly proportional to the mass velocity, and inverse proportional to length-to-diameter ratio. A simple dimension correlation for CHF of cyclohexane in the study was fitted as Eq. (4), in which constant efficient $C = 139.9$ kJ/kg. Furthermore, it was found through the transformation of Eq. (4) that enthalpy rise of cyclohexane at CHF condition equals 4C, seen in Eq. (5). Fig. 8 shows that almost all the CHF data points can be well predicted with the error range of ±15% and RMS error of 8.1%. This means that Eq. (5) can be used to predict CHF and critical vapor quality qualitatively. According to the correlation fitted, CHF occurred at nearly constant fluid enthalpy with deviation of ±15%.

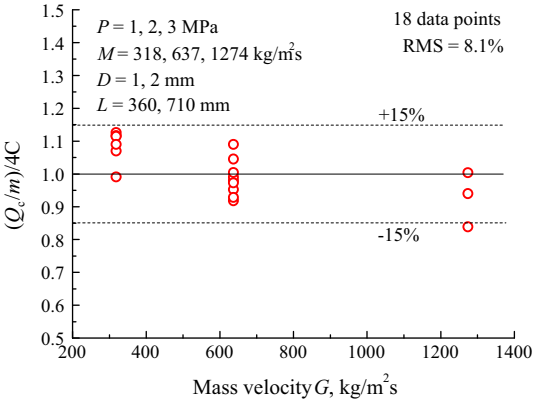

Fig. 8. Verification of the CHF correlation fitted for cyclohexane.

$$q_c = C\frac{GD}{L} \quad (C = 139.9\ \text{kJ/kg}) \tag{4}$$

$$h = \frac{Q_c}{m} = \frac{4q_c \cdot \pi DL}{G \cdot \pi D^2} = \frac{4q_c L}{GD} = 4C \tag{5}$$

However, the range of ±15% with interval of 168 kJ/kg is a big enthalpy difference for cyclohexane. The latent heat of vaporization is (265.4, 203.1 and 141.3) kJ/kg at pressure of (1, 2 and 3) MPa respectively. The critical vapor quality will be predicted in the range of $0.42 < x_c < 1.05$ when $P = 1$ MPa, $-0.07 < x_c < 0.75$ when $P = 2$ MPa, and $-0.79 < x_c < 0.40$ when $P = 3$ MPa. It can be clearly seen that nearly all the critical vapor quality values of experimental CHF point well located in the predicted region. And it has given an explanation for that the critical qualities shifted to the lower value region at higher pressure, shown in Figs. 4 and 5. The reason is that the less latent heat of vaporization at higher pressure leads to the lower critical vapor quality at the nearly constant fluid enthalpy region for CHF.

3.7. Comparison of the CHF data with existed correlations

One of the most widely used correlations developed for saturated CHF in a single channel is the Katto–Ohno [5] correlation. For no inlet liquid subcooling, they correlated CHF as formula (6).

$$\frac{q_{co}}{Gh_{lv}} = f\left[\frac{\rho_l}{\rho_v}, \frac{\sigma\rho_l}{G^2L}, \frac{L}{D}\right] \tag{6}$$

For most regimes, they found a linear rise in CHF with increasing inlet liquid subcooling. Therefore, subcooling was taken into account by the Eq. (7), where q_c is the CHF for conditions with inlet liquid subcooling, q_{co} is the CHF for inlet saturation conditions, Δh_i is the inlet enthalpy of subcooling with respect to saturation and K is an empirical inlet subcooling parameter.

$$q_c = q_{co}\left(1 + K\frac{\Delta h_i}{h_{lv}}\right) \tag{7}$$

Qu and Mudawar [3] found that this correlation is fairly accurate at predicting saturated CHF in single circular mini-channels.

Cyclohexane entered the test channel at ambient temperature of approximately 20 °C. The high inlet subcooling of (162.1, 206.4, and 236.3) °C was taken into account by Eq. (7) at pressures of (1, 2 and 3) MPa respectively. In order to evaluate the effect of inlet subcooling, the critical heat flux was calculated by not considering the inlet subcooling, shown in Fig. 9. It can be seen that the predicted q_c deviates the experimental q_c with MAE of 68.7%, and

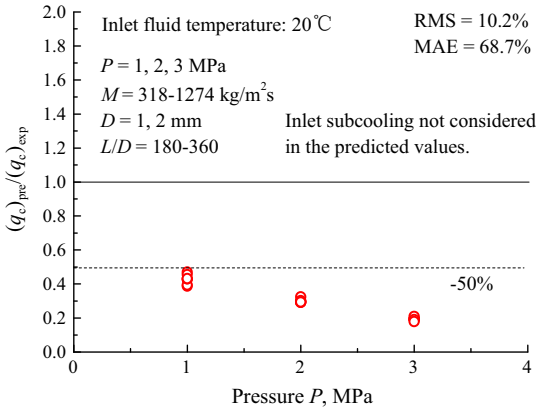

Fig. 9. Effect of inlet subcooling on CHF.

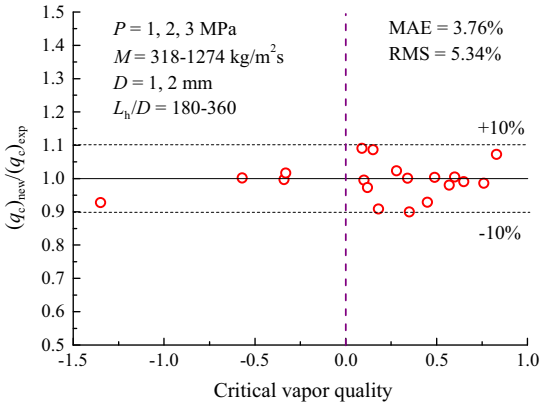

Fig. 11. Comparison of the experimental CHF data with those predicted by the new correlation.

bigger errors produced at bigger subcooling condition with bigger pressure.

Inlet subcooling is a significant effect on CHF. According to Katto–Ohno correlation, effect of inlet subcooling on CHF is mainly considered in the correlation as the ratio of inlet enthalpy of subcooling to the latent heat of vaporization $\Delta h_i/h_{lv}$. However, the inlet subcooling of (2–10) °C for R134a was indicated to have no influences on CHF in previous literature [11]. In fact, the inlet subcooling of (2–10) °C which produced limited effect to be hardly observed. But, in this study the conditions are completely different. Ambient temperature of 20 °C in the inlet means inlet enthalpy of subcooling of (364, 490 and 587) kJ/kg, which are 137%, 241% and 415% of the latent heat of vaporization at pressure of (1, 2 and 3) MPa respectively. And it gives the explanation that bigger deviations produced at higher pressure condition with inlet subcooling not considered.

Comparisons of experimental CHF data with those predicted by the Katto–Ohno correlation [5] and shah correlation [10] with inlet subcooling considered are shown in Fig. 10 at (a) different pressures and (b) different critical vapor qualities. Good agreements were achieved between the experimental CHF and the predicted values, for Katto–Ohno correlation the mean average error MAE = 20.5% and RMS error = 9.0%, and for Shah correlation MAE = 15.0% and RMS error = 13.6%. For both correlations, most of the data points are in the deviation of 30%.

The comparison at different critical vapor qualities showed that both the correlations can predict the subcooled CHF with the same deviations for the saturated CHF.

3.8. Corrected CHF correlation for cyclohexane

An improved CHF correlation, based on the Katto–Ohno [5] CHF correlation, is developed below to fit the current CHF experimental data. For CHF of inlet saturation condition, the Katto–Ohno CHF correlation is directly used without any correction. And a new equation is proposed to consider the subcooling by the Eq. (8), where q_c is the CHF for conditions with inlet liquid subcooling, q_{co} is the CHF for inlet saturation conditions, Δh_i is the inlet enthalpy of subcooling with respect to saturation.

$$q_c = q_{co}\left(1 + 0.9952\frac{\Delta h_i}{h_{lv}}\right) \tag{8}$$

Comparison of the experimental CHF data with the values predicted by new correlation was shown in Fig. 11. Excellent agreements were achieved between the experimental data and the predicted values with MAE = 3.76%, and RMS error = 5.34%. The deviations of all the experimental data including the saturated CHF and the subcooled CHF were in the range of ±10%. It indicated that the new correlation developed is validated and very accurate for both saturated CHF and subcooled CHF in the corresponding parameters range of this paper.

4. Conclusions

CHF of cyclohexane flow boiling was experimentally investigated in uniformly heated minichannels. Highly subcooled

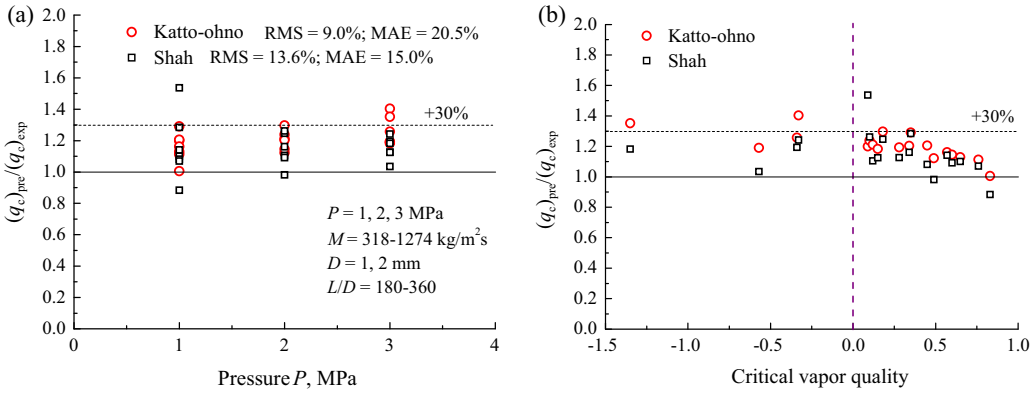

Fig. 10. Comparison of experimental CHF with Katto–Ohno correlation and Shah correlation for (a) different pressures and (b) different critical vapor qualities.

cyclohexane entered the test channel at ambient temperature of approximately 20 °C. It concluded:

(1) CHF of cyclohexane was obtained at different channel diameters, heated lengths, mass velocities and pressures. As heat flux continued to increase after the occurrence of CHF, dryout location shifted toward the front of the channel with lower vapor quality and higher post-dryout wall temperature.
(2) Parameter effects on CHF of cyclohexane were investigated. CHF increased with an increase in mass flux, and decreased with an increase in length-to-diameter ratio. Reducing channel diameter from 2 mm to 1 mm at the same length-to-diameter ratio was proved to have no significant effects on CHF values of cyclohexane at the tested conditions. CHF values increased with an increase in pressure at higher mass velocities, and no pressure effects were observed at lower mass velocities. However, the critical vapor quality decreased with an increase in pressure in all the conditions, especially for smaller diameter channel the critical vapor quality reduced more rapidly.
(3) CHF of cyclohexane was fitted to be proportional to mass flux and inverse proportional to length-to-diameter ratio. Good agreement was achieved between the CHF experimental data and those predicted by Katto–Ohno correlation (MAE = 20.5%) and Shah correlation (MAE = 15.0%) for whatever saturated CHF or subcooled CHF. A corrected Katto–Ohno CHF correlation was developed to fit the current experimental data. Excellent agreement was obtained between the experimental data and those predicted by the corrected CHF correlation with MAE = 3.76%, and RMS error = 5.34%. And the deviations of all the experimental data are in the range of ±10%.

Acknowledgments

This work is sponsored by National Natural Science Foundation of China (Grant No. 21306147), China Postdoctoral Science Foundation (Grant No. 2013M532044) and Fundamental Research Funds for the Central Universities. Their financial supports are grateful acknowledged.

References

[1] I. Mudawar, Assessment of high-heat-flux thermal management schemes, IEEE Trans. Compon. Pack. Technol. 24 (2001) 122–141.
[2] Stiegemeier B, Meyer ML, Taghavi R. A thermal stability and heat transfer investigation of five hydrocarbon fuels: JP-7, JP-8, JP-8+100, JP-10, and RP-1. In: 38th AIAA/ASME/SAE/ASEE joint propulsion conference & exhibit, Indiana, USA, AIAA 2002-3837; 2002.
[3] W. Qu, I. Mudawar, Measurement and correlation of critical heat flux in two-phase microchannel heat sinks, Int. J. Heat Mass Transfer 47 (2004) 2045–2059.
[4] A. Kosar, Y. Peles, Critical heat flux of R-123 in silicon-based microchannels, J. Heat Transfer 129 (2007) 844–851.
[5] Y. Katto, H. Ohno, An improved version of the generalized correlation of critical heat flux for the forced convective boiling in uniformly heated vertical tubes, Int. J. Heat Mass Transfer 27 (9) (1984) 1641–1648.
[6] C. Tibiriçá, S. Szczukiewicz, G. Ribatski, J.R. Thome, Critical heat flux of R134a and R245fa inside small-diameter tubes, Heat Transfer Eng. 34 (5) (2013) 492–499.
[7] C. Konishi, I. Mudawar, M.M. Hasan, Investigation of localized dryout versus CHF in saturated flow boiling, Int. J. Heat Mass Transfer 67 (2013) 131–146.
[8] A. Kosar, C.J. Kuo, Y. Peles, Suppression of boiling flow oscillations in parallel microchannels with inlet restrictors, J. Heat Transfer 128 (2006) 251–260.
[9] Y. Katto, A generalized correlation of critical heat flux for the forced convection boiling in vertical uniformly heated round tubes, Int. J. Heat Mass Transfer 21 (1978) 1527–1542.
[10] M. Shah, Improved general correlation for critical heat flux during upflow in uniformly heated vertical tubes, Int. J. Heat Fluid Flow 8 (1987) 326–335.
[11] L. Wojtan, R. Revellin, J.R. Thome, Investigation of saturated critical heat flux in a single uniformly heated microchannel, Exp. Therm. Fluid Sci. 30 (2006) 765–774.
[12] W. Zhang, T. Hibiki, K. Mishima, et al., Correlation of critical heat flux for flow boiling of water in mini-channels, Int. J. Heat Mass Transfer 49 (2006) 1058–1072.
[13] A.P. Roday, M.K. Jensen, Study of critical heat flux condition with water and R-123 during flow boiling in microtubes. Part I: Experimental results and discussion of parametric effects, Int. J. Heat Mass Transfer 52 (2009) 3235–3249.
[14] Z. Wu, W. Li, S. Ye, Correlations for saturated critical heat flux in microchannels, Int. J. Heat Mass Transfer 54 (2011) 379–389.
[15] A. Tanase, S.C. Cheng, D.C. Groeneveld, et al., Diameter effect on critical heat flux, Nucl. Eng. Des. 239 (2009) 289–294.
[16] D.C. Groeneveld, J.Q. Shan, A.Z. Vasic, et al., The 2006 CHF look-up table, Nucl. Eng. Des. 237 (2007) 1922–1999.
[17] C.L. Ong, J.R. Thome, Macro-to-microchannel transition in two-phase flow: Part 2–Flow boiling heat transfer and critical heat flux, Exp. Therm. Fluid Sci. 35 (6) (2011) 873–886.
[18] Shi Y, Yuan K, Zhao X, et al. Study on comparison between Inconel 617 and GH3128 as structural material candidates for intermediate heat exchanger. In: Proceedings of the 2013 21st international conference on nuclear engineering, ICONE21–15948, July 29-August 2, 2013, Chengdu, China.
[19] Z. Liu, Q. Bi, Y. Guo, et al., Heat transfer characteristics during subcooled flow boiling of a kerosene kind hydrocarbon fuel in a 1 mm diameter channel, Int. J. Heat Mass Transfer 55 (2012) 4987–4995.
[20] Z. Liu, Q. Bi, Y. Guo, et al., Convective heat transfer and pressure drop characteristics of near-critical-pressure hydrocarbon fuel in a mini-channel, Appl. Therm. Eng. 51 (2013) 1047–1054.
[21] Z. Liu, Q. Bi, Y. Guo, et al., Hydraulic and thermal effects of coke deposition during pyrolysis of hydrocarbon fuel in a mini-channel, Energy Fuels 26 (6) (2012) 3672–3679.
[22] J.R.S. Thom, W.M. Walker, et al., Boiling in subcooled water during flow up heated tubes or annuli, Proc. Inst. Mech. Eng. 180 (1966) 226–246.
[23] V. Kefer, W. Kohler, W. Kastner, Critical heat flux (CHF) and poat-CHF heat transfer in horizontal and inclined evaporator tubes, Int. J. Multiphase Flow 15 (3) (1989) 385–392.